SCIENTIFIC REPORTS

OPEN

SUBJECT AREAS:
BIOMEDICAL MATERIALS
ELECTRONIC PROPERTIES AND DEVICES

Received
27 January 2014

Accepted
25 February 2014

Published
12 March 2014

Correspondence and requests for materials should be addressed to Z.F.D. (zfdi@mail.sim.ac.cn) or X.Y.L. (xyliu@mail.sic.ac.cn)

* These authors contributed equally to this work.

Antibacterial activity of large-area monolayer graphene film manipulated by charge transfer

Jinhua Li[1]*, Gang Wang[2,3]*, Hongqin Zhu[1], Miao Zhang[2], Xiaohu Zheng[2], Zengfeng Di[2], Xuanyong Liu[1] & Xi Wang[2]

[1]State Key Laboratory of High Performance Ceramics and Superfine Microstructure, Shanghai Institute of Ceramics, Chinese Academy of Sciences, Shanghai 200050, China, [2]State Key Laboratory of Functional Materials for Informatics, Shanghai Institute of Microsystem and Information Technology, Chinese Academy of Sciences, Shanghai 200050, China, [3]School of Physical Science and Technology, Lanzhou University, Lanzhou 730000, China.

Graphene has attracted increasing attention for potential applications in biotechnology due to its excellent electronic property and biocompatibility. Here we use both Gram-positive Staphylococcus aureus (S. aureus) and Gram-negative Escherichia coli (E. coli) to investigate the antibacterial actions of large-area monolayer graphene film on conductor Cu, semiconductor Ge and insulator SiO_2. The results show that the graphene films on Cu and Ge can surprisingly inhibit the growth of both bacteria, especially the former. However, the proliferation of both bacteria cannot be significantly restricted by the graphene film on SiO_2. The morphology of S. aureus and E. coli on graphene films further confirms that the direct contact of both bacteria with graphene on Cu and Ge can cause membrane damage and destroy membrane integrity, while no evident membrane destruction is induced by graphene on SiO_2. From the viewpoint of charge transfer, a plausible mechanism is proposed here to explain this phenomenon. This study may provide new insights for the better understanding of antibacterial actions of graphene film and for the better designing of graphene-based antibiotics or other biomedical applications.

Graphene has a unique two-dimensional (2D) hexagonal lattice structure of sp^2 hybridized carbon atoms[1–3]. Compared to other carbon allotrope, i.e., fullerenes, carbon nanotubes and graphite, graphene exhibits many exceptional physical and chemical properties. For example, in single-layer graphene, electrons can behave as massless Dirac fermions[4]. Owing to these unique properties and biocompatibility, graphene has attracted widespread attention for numerous potential applications in biotechnology[5–7]. The destructive interactions of graphene and microbes have been widely investigated[8–12]. Fan's group had firstly found that graphene oxide (GO) possessed excellent antimicrobial activity in 2010[8]. Since then, Akhavan further investigated that both GO and reduced GO (rGO) nanowalls could be effectively against Gram-negative and Gram-positive microbes through direct contact, and rGO exhibited stronger antimicrobial activity than GO[9]. These rGO nanosheets can suppress the proliferation of microbes on their surfaces even in an environment that is highly suitable for microbial growth[10]. Tour's group reported that GO can perform as a terminal electron acceptor for environmental microbes, which provides a promising insight for its bioremediation[11]. The antimicrobial activity of GO and rGO are attributed to the sharp edge effect via a direct contact in these works. A recent work has confirmed that these GO and rGO nanosheets can extract phospholipids from Escherichia coli membranes and destroy the membrane integrality, thus killing Escherichia coli[13]. These works well explained the antibacterial actions of GO and rGO nanosheets. The destruction effect due to graphene nanosheet edges is expected to be significantly restricted when graphene nanosheets merge together to form large-area graphene film. So far, to the best of our knowledge, few studies reported on the antibacterial actions of chemical vapor deposited graphene film that is of large area and structural flatness.

Considering the practical applications of CVD-derived graphene films will combine with different substrates which can be classified into three ones by electrical characteristics, i.e., conductor, semiconductor, and insulator, herein, we fabricate three types of large-area monolayer graphene films on conductor Cu, semiconductor Ge (using APCVD method) and insulator SiO_2 (transferred from the graphene grown on Ge) substrates. Both Gram-negative Escherichia coli and Gram-positive Staphylococcus aureus are used to investigate their responses to the graphene film on conductor Cu, semiconductor Ge and insulator SiO_2. It is observed that graphene film on

different substrates shows different antibacterial actions. The antibacterial mechanism of the graphene film on various substrates was discussed based on their charge transfer capability. To the best of our knowledge, such an interaction of microbes with graphene films on different substrates, that is, conductor, semiconductor and insulator, has not been reported previously, and the findings may offer new insights both for the better understanding of antibacterial actions of graphene films and for the better designing of graphene-based antibiotics or other biomedical applications.

Results

Fabrication and characterization of graphene film. Atmospheric pressure chemical vapor deposition (APCVD) method was used to grow large-area graphene films on Cu and Ge substrates (denoted as Graphene@Cu and Graphene@Ge, respectively). Figure 1a–d represents the X-ray photoelectron spectroscopy (XPS) analysis results acquired from the Graphene@Cu and Graphene@Ge surfaces. The XPS depth profile in Figure 1a reveals the limited carbon dissolution and diffusion in the Cu substrate after the growth of graphene film, which is similar to that of the Ge substrate in Figure 1c. Therefore, it suggests that the CVD growth of graphene on either Cu substrate or Ge substrate proceeds via self-limiting and surface-mediated process rather than surface segregation, which is responsible for Ni-catalyzed growth of graphene[14]. Figure 1b and d shows the XPS full spectra from Graphene@Cu and Graphene@Ge surfaces, respectively, and the insets in Figure 1b and d are the corresponding C1s spectra of graphene films on Cu and Ge substrates. Secondary ion mass spectrometry (SIMS) analysis was also performed on Graphene@Cu and Graphene@Ge surfaces. The results are given in Figure S1, which was consistent with the XPS analysis. Based on these analysis results, the monolayer graphene film on Ge substrate behaves as an analogue of that on Cu substrate[15].

To evaluate the crystalline quality of the obtained graphene films and determine the layer number, graphene films were transferred from the Cu and Ge substrates onto transmission electron microscopy (TEM) grids via a PMMA-assisted wet-transfer method (Supplementary experimental details). The graphene films, transferred from either Cu substrate or Ge substrate, appear continuous

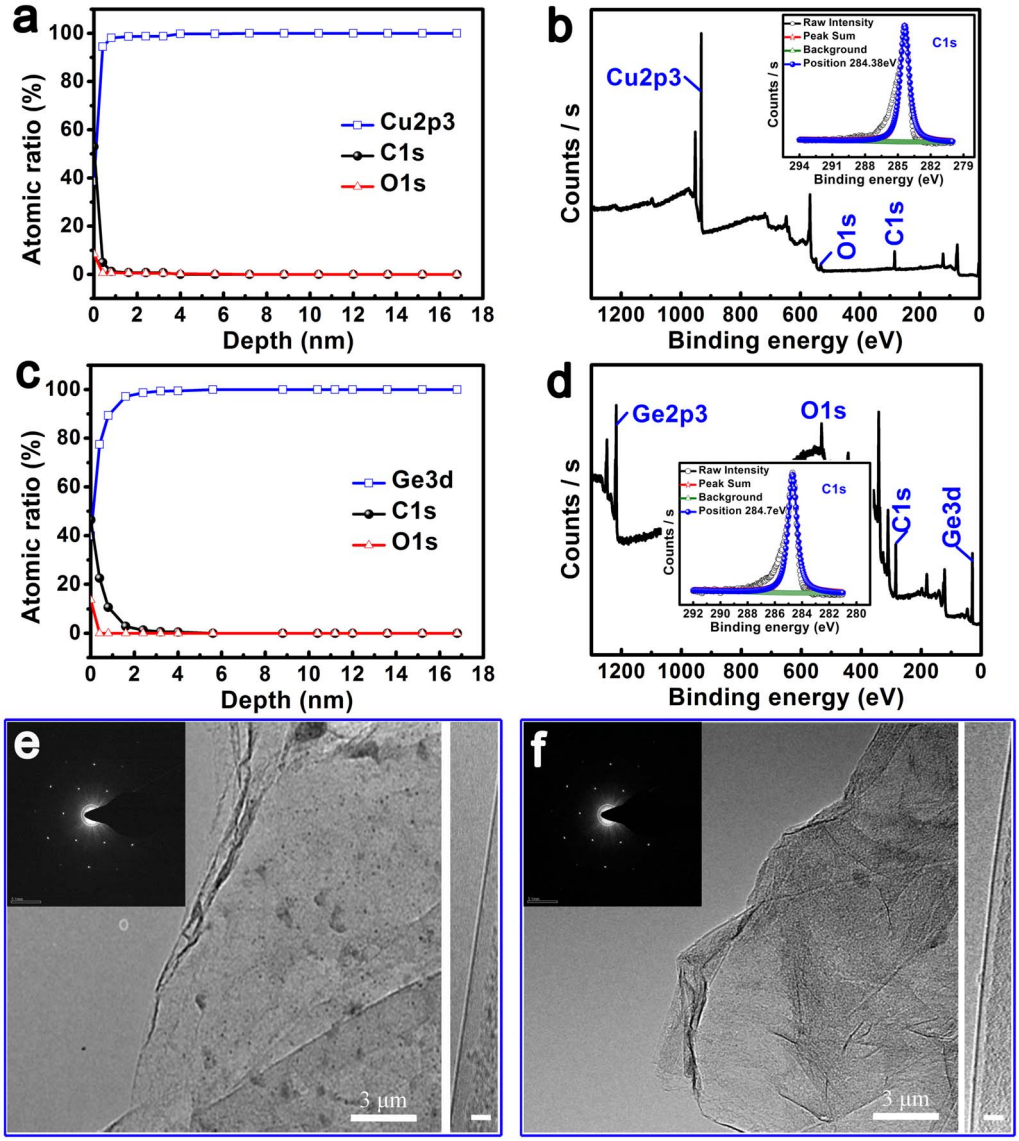

Figure 1 | (a and c) XPS depth profiles of carbon distribution in Cu (a) and Ge (c) substrates after the growth of graphene films, accompanied by the corresponding XPS full spectra of graphene film-coated Cu (b) and Ge (d) surfaces. The insets in (b) and (d) are the corresponding C1s XPS spectra of graphene films on Cu and Ge; (e and f) TEM images and the inserted SAED patterns of the transferred graphene films from Cu (e) and Ge (f) substrates, respectively. The right insets in (e) and (f) are the corresponding HRTEM images of monolayer graphene edge that show one carbon layer, with a scale bar of 3 nm.

over large area (Figure 1g and h). And, the corresponding selected area electron diffraction (SAED) patterns exhibit only one set of hexagonal diffraction pattern which suggest both two graphene films are monolayered and possess the high crystalline quality. Furthermore, the monolayer feature of the obtained graphene films has been verified by the high-resolution TEM images in Figure 1g and h randomly taken from the graphene edges as well. The transmittance analysises also suggest the obtained graphene films, either on Cu substrate or Ge substrate, are monolayered (Supplementary Figure S2).

Uniformity and coverage of graphene film. Beside the above-mentioned Graphene@Cu and Graphene@Ge, Graphene@SiO_2 which is obtained by the transfer of graphene film grown on Ge onto SiO_2 substrate, is also included for comparison, as illustrated in Figure 2a. To ensure the validity of the antibacterial test, the testing graphene film specimens must be large-area and homogeneous. Figure S3 shows the photographs of the large-area graphene films on Cu, Ge and SiO_2. As shown in Figure 2b, the Raman spectra acquired from the surfaces of Graphene@Cu, Graphene@Ge, and Graphene@SiO_2 present huge similarity. The typical features of graphene, i.e., the 2D band at ~2710 cm^{-1} and the G band at ~1580 cm^{-1}, intensively appeared. Meanwhile, very little defect related to the D band emerged near 1350 cm^{-1}, indicating the high quality of the graphene films on these substrates. The attenuation of the D band also indicates the high crystallinity of the obtained graphene films. Differing from the graphene nanosheets, Graphene@Cu, Graphene@Ge and Graphene@SiO_2 are expected to be continuous over large area. To estimate the uniformity and the coverage of the as-prepared graphene films on conductor Cu, semiconductor Ge and insulator SiO_2 substrates, 25 points that are uniformly distributed over the area of 1 cm × 1 cm have been analyzed by Raman scattering, as shown in Figure 2c. Using the software named Wafer Viewer, the I_{2D}/I_G ratio mapping of graphene films coated on Cu, Ge and SiO_2 substrates are given at both low magnification and high magnification. The I_{2D}/I_G ratios

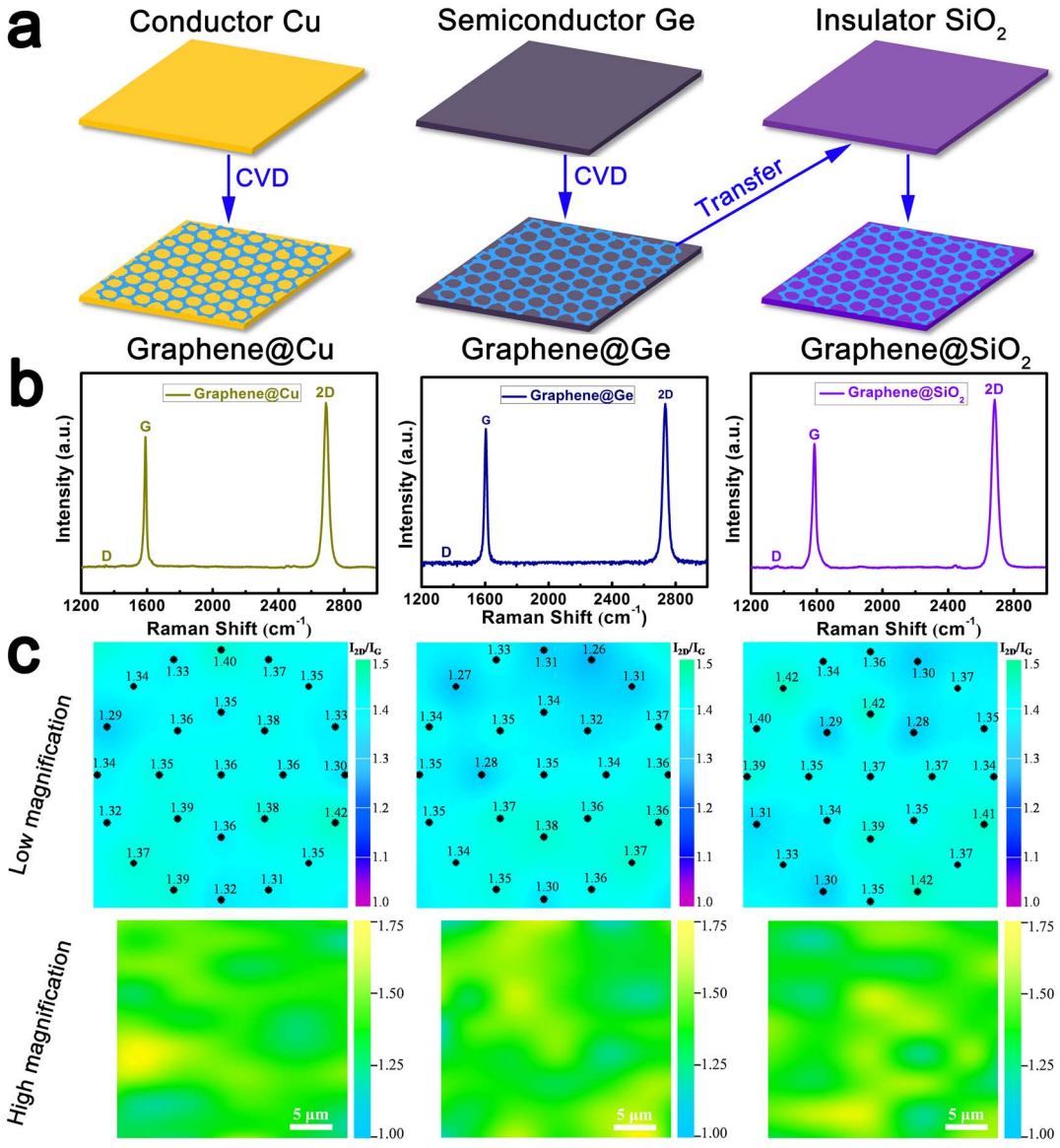

Figure 2 | (a) Schematic illustration for the fabrication of the testing graphene film samples, i.e., large-area monolayer graphene films on conductor Cu, semiconductor Ge and insulator SiO_2 substrates; (b) Raman spectra of the graphene films on Cu, Ge and SiO_2 substrates, respectively; (c) Raman mapping results of the monolayer graphene films on Cu, Ge and SiO_2 substrates at both low and high magnification, showing the uniformity and the coverage of the as-grown monolayer graphene films on these substrates. The Raman mapping area at low magnification is 1 × 1 cm^2, as illustrated in Supplementary Figure S4.

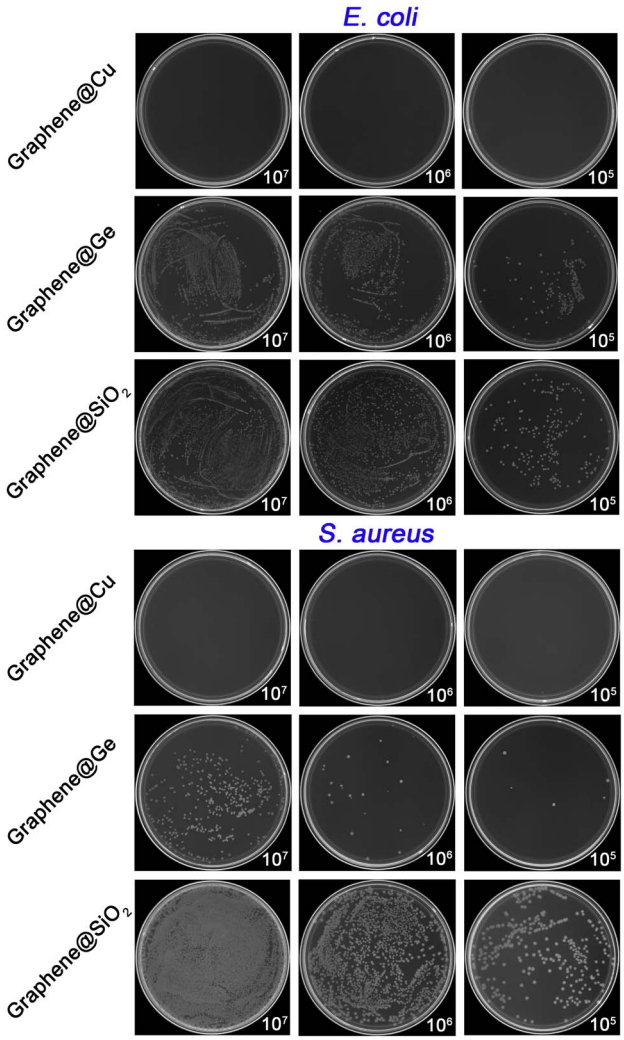

Figure 3 | Typical photographs of re-cultivated E. coli colonies (top panel) and S. aureus colonies (bottom panel) on agar culture plates, with the seeded concentrations of bacteria onto graphene films being 10^7 CFU/mL, 10^6 CFU/mL and 10^5 CFU/mL, respectively.

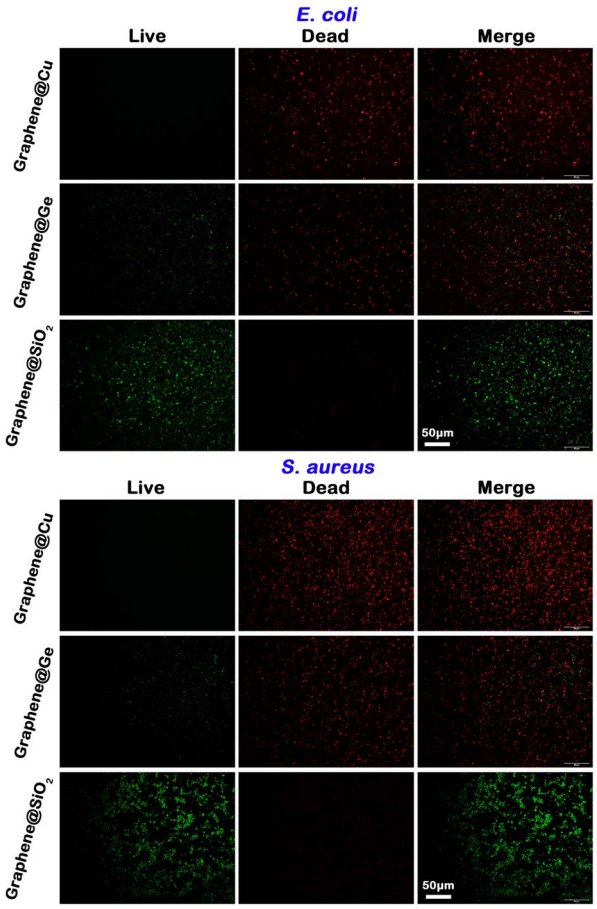

Figure 4 | **Representative fluorescence images showing the viability of the bacteria on graphene film samples after 24 hours of incubation, visualized by staining with a LIVE/DEAD® BacLight™ Bacterial Viability Kit (L13152).** The live bacteria appear green while the dead ones are red. The seeded concentration of bacteria onto the graphene films is 10^7 CFU/mL.

calculated from the 25 points are in the range of 1.2 to 1.4, indicating the graphene films coated on Cu, Ge and SiO_2 substrates are quite uniform at the corresponding scale. And the I_{2D}/I_G ratios from the randomly selected areas at high magnification further demonstrated the high quality of these graphene films on substrates.

Bacterial response to graphene film. In order to investigate the responses of both Gram-negative Escherichia coli (E. coli) cells and Gram-positive Staphylococcus aureus (S. aureus) cells to the graphene films on different substrates, i.e., Graphene@Cu, Graphene@Ge and Graphene@SiO_2, the attached bacteria were dissociated from the surfaces, re-cultivated on agar, and evaluated by using the bacteria counting method. Figure 3 gives the typical photographs of E. coli or S. aureus bacteria colonies number on three types of graphene films starting with various concentrations of bacteria. As can be seen from the top panel of this figure, for Graphene@Cu, at each concentration of E. coli, there were no bacteria colonies on the agar, significantly indicating that the E. coli cells cannot survive on the graphene film. When culturing the E. coli on Graphene@Ge surface, the re-cultivated bacteria colonies can be seen clearly on the agar at each concentration of bacteria. In regard to the Graphene@SiO_2, continuous bacteria colonies were prevalent on the agar culture medium, implying that the E. coli cells can well survive on the Graphene@SiO_2 surface. The similar phenomena are observed for the S. aureus cultured on the Graphene@Cu, Graphene@Ge, and Graphene@SiO_2 surfaces. Besides, for each initial bacteria concentration, the S. aureus cells seem to show more susceptive toward the different graphene/substrate systems compared to the E. coli cells.

Fluorescence staining was also used to visualize and to verify the capability of the graphene films to fight against viable bacteria colonization. The results are shown in Figure 4. After 24 hours of incubation, there are large amounts of viable bacteria (green) on the Graphene@SiO_2 surface. On the contrary, the amounts of viable bacteria are evidently lower on the Graphene@Cu and Graphene@Ge surfaces and in particular, nearly no viable bacteria can be observed on Graphene@Cu. The observed distinct results were further investigated by the SEM analysis to validate the potential antibacterial actions, including bacteriostatic action and bactericidal action. SEM observation was utilized to identify the morphology and membrane integrity of both the E. coli and S. aureus cells, as shown in Figure 5. In detail, as shown in the top panel of Figure 5, for the E. coli cultured on Graphene@Cu, every bacterial cell in the visible field at low magnification was suffered from a severe membrane disruption and cytoplasm leakage, indicated by the white arrow at high magnification. It should be noted that the possible interference to the antibacterial activity of the Graphene@Cu caused by Cu ions release has been totally precluded, since the inductively-coupled plasma mass spectrometry (ICP-MS) analysis reveals that no copper ions were released when the Graphene@Cu was immersed in physiological saline (0.9 wt% NaCl aqueous solution) for 72 h. In

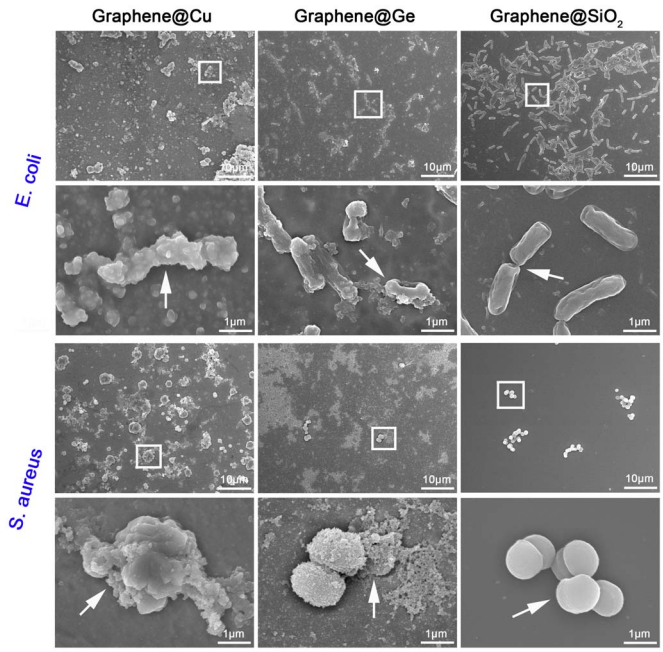

Figure 5 | SEM morphology of the E. coli cells (top panel) and the S. aureus cells (bottom panel) that were seeded onto the graphene films at both low and high magnification, with the seeded concentration of bacteria being 10^7 CFU/mL. The white arrows at high magnification correspond to the rectangular areas at low magnification, respectively.

fact, it has been reported that the CVD-deposited graphene film on Cu substrate can act as an efficient diffusion barrier, thus protecting the underlying Cu against hot O_2 oxidation, hot H_2O_2 aqueous solution corrosion[16], or the electrochemical degradation[17]. As for the Graphene@Ge, prevalent membrane damage and cytoplasm leakage can be still found everywhere in the visible field. It was also observed that some bacterial cells still had maintained the membrane integrity, but they were out of shape, showing their poor living state. With regard to the graphene film on SiO_2, a lot of E. coli bacteria can be seen at low magnification. Randomly selecting an individual bacterium to magnify, one can find that intact cytoplasmic membrane was protecting the bacterium. Besides, intercellular communication can also be found here and there, which indicated their exuberant vitality[18]. As a result, the E. coli cells cultured on Graphene@SiO_2 surface showed no significant membrane damage and cell death, indicating that the surface of Graphene@SiO_2 cannot significantly destroy the E. coli microbes. The SEM analysis results were quite consistent with the bacteria colonies number results in Figure 3. These were also true for the S. aureus cells cultured on the graphene films (the bottom panel of Figure 5). Prevalent cell lysis and cytoplasma leakage were observed on both the Graphene@Cu and Graphene@Ge surfaces, especially on the Graphene@Cu without an intact S. aureus cell in the visible field at low magnification, while still some individual bacteria remained the membrane integrity despite their poor living state on Graphene@Ge. The results indicate that the S. aureus bacteria can hardly survive on both the surfaces. However, the S. aureus cells on Graphene@SiO_2 surface showed no severe membrane disruption. These observed results also agreed well with the bacteria colonies number results in Figure 3. Besides, from the SEM observation, the number of the attached S. aureus bacteria onto the graphene films was lower than that of the attached E. coli bacteria, implying a higher susceptibility. The obtained results reveal that the death of both the Gram-negative E. coli cells and the Gram-positive S. aureus cells on Graphene@Cu and Graphene@Ge surfaces can be ascribed to the disruption of their microbial membrane integrity and the leakage of their cytoplasma content.

Discussion

Bacteria carry out respiration to produce energy for vital movement, such as cell growth and maintenance[19,20]. This process requires extracellular electron acceptors to realize electron transport in respiratory chain[21]. From the view of endosymbiotic theory, a microbial cell is similar to the mitochondrion of a mammalian cell. There is an electron conduit based on respiratory proteins between the microbial membranes and the extracellular environment to produce energy[22]. According to a previous work, these respiratory proteins may possess semiconductivity with a bandgap of 2.6 eV to 3.1 eV[23]. Thus, we hypothesize that the respiratory proteins may behave as n-type semiconductors. The physical contact of microbes with semimetal graphene will result in Schottky barrier formation and Fermi level alignment based on the band theory, which bring the facile transfer of electrons from microbial membranes to graphene acceptors. In fact, graphene is an excellent electron acceptor[14,24,25]. On the other hand, microbial cells maintain a negative resting membrane potential in the range of −200 mV to −20 mV[26]. If a graphene-on-substrate junction can form a circuit for electron transfer, one can easily speculate that the microbial membranes may steadily lose electrons under the negative membrane potential. Therefore, the conductivity, in other words, the band structure of the underlying substrates may play an important role in microbial responses.

Here, the ground serves as a reference of zero potential. A schematic circuitry is depicted in Figure 6a for the contact of microbes, graphene films and the underlying substrates. To illustrate the proposed mechanism for the observed phenomena of microbial responses to the graphene film on conductor Cu, semiconductor Ge and insulator SiO_2 substrates, the energy band diagrams of these graphene-on-substrate junctions are depicted in Figure 6b–d. Some data in early works[27–32], as well as some calculated values here, are used to draw the band structures, as listed in Table 1. Figure 6b gives the band structure of the Membrane@Graphene@Cu contact. From this figure, it can be seen that the electrons are easily transferred from microbial membrane to graphene film and then to the underlying conductor Cu substrate, which forms a circuit for electron transfer. The membrane electrons are extracted by the graphene film on Cu quickly and potently, until the bacterial cell loses its viability. As a result, no bacteria can survive on the graphene film, as shown in Figure 3 to Figure 5. For the Membrane@Graphene@Ge contact, as shown in Figure 6c, the electrons can also be transferred from microbial membrane to graphene film and then to the underlying semiconductor Ge substrate, which also forms a circuit for electron transfer. It is noted that, this electron extraction ability is less strongly than the graphene film on Cu, due to the semiconductivity. So, although the graphene film on Ge can kill most bacteria, there are still some individual ones maintaining membrane integrity in a poor living state. However, for the Membrane@Graphene@SiO_2 contact, the electrons cannot be transferred to the underlying insulator SiO_2 substrate, which thus cannot form a circuit for electron transfer, as shown in Figure 6d. As a result, the bacteria can survive on the graphene film and not be killed.

Hence, for both the conductor Cu and the semiconductor Ge substrates, the graphene-on-substrate junctions can act as an electron pump. The electrons are steadily pumped away from the microbial membrane under the negative membrane potential, which produces a ROS-independent oxidative stress to the microbial membrane. In this way, the electron transport in membrane respiratory chain may be interrupted by the direct contact with graphene films on conductor Cu and semiconductor Ge substrates, which eventually causes the destruct of microbial membrane integrity and the death of microbial cells. Meanwhile, the interruption of the electron transport in membrane respiratory chain elicits a rapid depletion of the levels of intracellular ATP[33]. The depletion of ATP levels may be a stimulation of hydrolysis of residual ATP in return, eventually culminating in the loss of cell viability. On the contrary, the Graphene@SiO_2

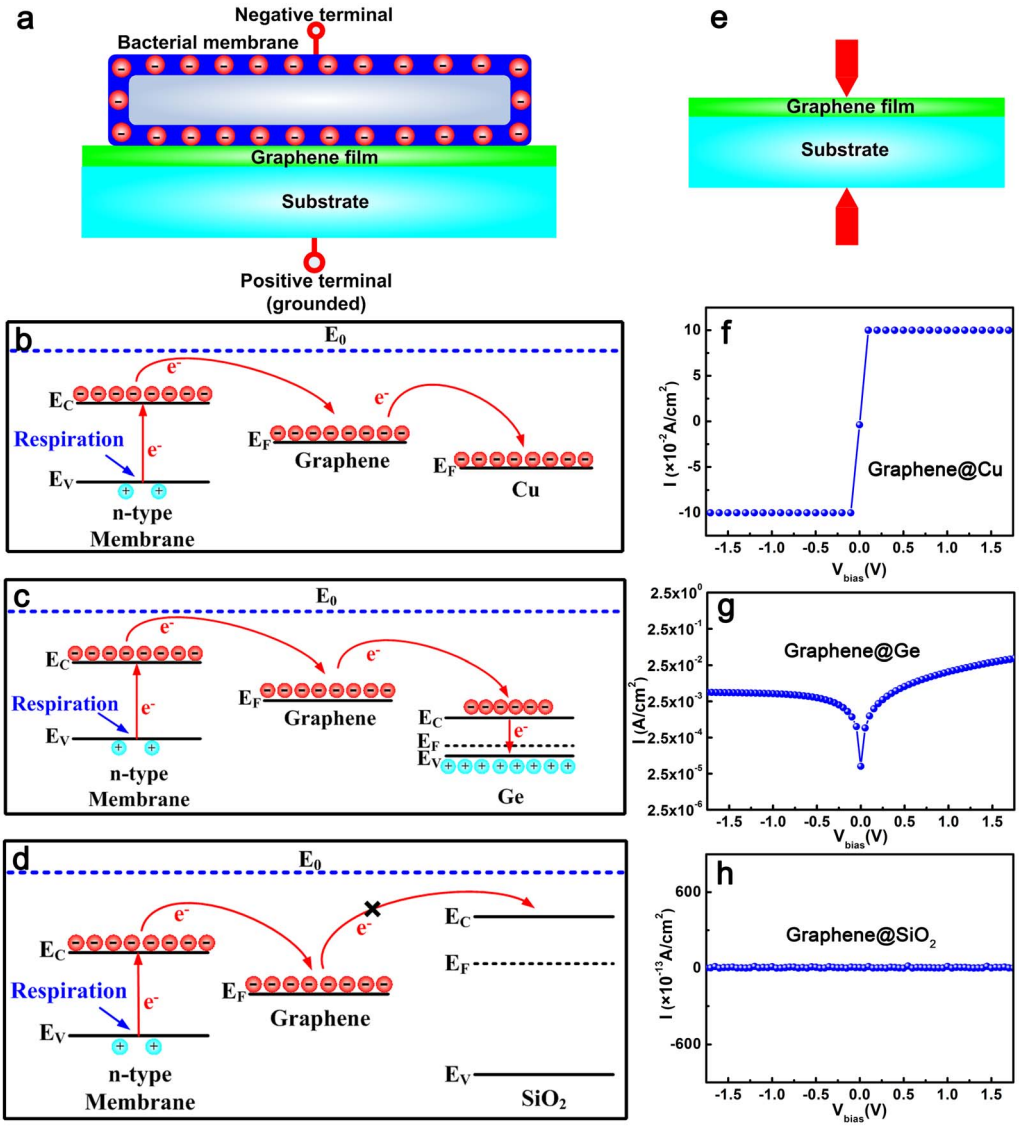

Figure 6 | (a–d) Schematic circuitry to illustrate the proposed mechanism for the observed phenomena of different responses of bacteria to the graphene films in darkness (a) on conductor Cu (b), semiconductor Ge (c) and insulator SiO_2 (d) substrates from the view of the energy band diagrams of these graphene-on-substrate junctions; (e–h) Schematic illustration for the electrical measurements (e) to obtain the current–voltage (I–V) characteristics of Graphene@Cu (f), Graphene@Ge (g) and Graphene@SiO_2 (h) contacts at room temperature, respectively, indicating three different contacts of graphene films with the underlying substrates.

surface does not possess a significant bactericidal activity toward both the Gram-negative E. coli cells and the Gram-positive S. aureus cells. The electrical properties measurements were also performed on the three types of graphene-on-substrate junctions, i.e., graphene-on-Cu, graphene-on-Ge and graphene-on-SiO_2, to analyze the I-V characteristics of these junctions and to further support the potential circuit for electron transfer. Figure 6e depicts the schematic illustration for the electrical measurements. The results are shown in Figure 6f–h. From this figure, one can clearly see that the graphene-on-Cu junction is just a conductor contact (Figure 6f) and the graphene-on-Ge junction exhibits a Schottky contact (Figure 6g). However, for the graphene-on-SiO_2 junction, it obviously presents an Ohmic contact (Figure 6h). Besides, the scanning tunneling microscope (STM) analysis may provide a potential support for the electron transfer between the bacterial membranes and the large-area monolayer graphene films on different substrates (Supplementary Figure S6).

Table 1 | Data for the energy level positions of Cu, Ge and SiO_2

Materials	Φ (eV)	E_g (eV)	χ (eV)	E_c (eV)	E_v (eV)
Cu	4.65[27]				
Ge	4.54[α]	0.63[α]	4[28]	−4[α]	−4.63[α]
SiO_2	3.03[29]	8.90[30]	0.9[α]	−0.9[31]	−9.8[α]
Graphene	4.23[29]				
Respiratory protein		2.6–3.1[23,32]			

Notes: E_0, vacuum level; E_F, Fermi level; Φ, work function; E_g, bandgap; χ, electron affinity; E_c, conduction band;
[α], Calculated values.

The membranes of Gram-negative E. coli cells are negatively charged, due to the isoelectric point pI = 4 ~ 5. For the Gram-positive S. aureus cells, the isoelectric point pI value of the membranes is 2 ~ 3, which produces a more negatively charged surface in culturing medium[34]. Therefore, the E. coli cells and the S. aureus cells have different surface electron states, which can contribute to the more resistance of E. coli cells against the direct contact interaction with graphene film on Cu, Ge or SiO_2 substrate than S. aureus cells,

thus accounting for the observed difference in the antimicrobial activity against Gram-negative E. coli and Gram-positive S. aureus.

So, the antibacterial activity of graphene does not stem from reactive oxygen species (ROS) mediated damage[35], but through electron transfer interaction from microbial membrane to graphene. This is similar for other carbon allotrope. The surface charge states of fullerene (C_{60}) nanoparticles determine the antimicrobial ability, independent of ROS[36]. Positively charged C_{60}-NH_2 can damage membrane integrity of Escherichia coli and Shewanella oneidensis. Neutrally charged C_{60} and C_{60}-OH only have mild adverse effect on the latter, while negatively charged C_{60}-COOH cannot affect the both[37]. Another work reported on the graphene-wrapped TiO_2 that highly enhanced the photocatalytic degradation of methylene blue (MB) under visible light irradiation, in which graphene bridged MB and TiO_2, and brought a faster charge transport rate of electrons[38].

Methods

CVD growth of graphene. The graphene films were grown on Cu substrates according to the previous work[15]. The growth of graphene on Ge substrates was carried out under atmospheric pressure according to our group's recent work[7]. The Ge substrates (175 μm in thickness, ATX) were cut into 1×1 cm^2 pieces and placed at the center of the horizontal quartz tube. The synthesis was carried out in a horizontal tube furnace inside a quartz processing tube (50 mm inner diameter). The quartz tube was evacuated to approximately 10^{-5} mbar and then filled with 200 standard cubic cm per min (sccm) Argon (Ar, 99.9999% purity) and 50 sccm Hydrogen (H_2, 99.9999% purity). After heating to the desired temperature (910°C), methane (CH_4) gas was introduced to deposit the graphene film for 100 min under ambient pressure. After deposition, the CH_4 gas was turned off and the furnace was cooled to room temperature under flowing H_2 and Ar.

Graphene transfer onto SiO_2. For the SiO_2 substrate, graphene films were transferred from the Ge substrate onto SiO_2 surface by a PMMA-assisted wet-transfer method. A thin layer of polymethyl methacrylate (MicroChem 950 PMMA C, 3% in chlorobenzene) was spin-coated onto the substrate to protect the graphene film and to act as a support which was then cured at 180°C for 10 min. Afterwards, the Ge substrate was etched away by a mixture of HNO_3 and HF (1 : 1) aqueous solution, allowing the PMMA/carbonic layer to float on top of the solution. After placing the layer on a filter paper, it was washed with deionized water. The PMMA/graphene layer was subsequently transferred onto SiO_2 substrate, followed by annealing at 50°C for 90 min to improve adhesion. The PMMA was then dissolved gradually with acetone and deionized water. Finally, the graphene sample was washed with isopropanol.

Characterization. The surface morphology was characterized by field emission scanning electron microscopy (FESEM; Magellan 400, FEI, USA). The chemical compositions and chemical states of the Ge surfaces were determined by X-ray photoelectron spectroscopy (XPS; PHI 5802, Physical Electronics Inc, Eden Prairie, MN). Raman spectroscopy (HORIBA Jobin Yvon HR800) was used to characterize the quality and uniformity of the grown graphene films at room temperature[39]. The Raman spectra were obtained using an Ar^+ laser with a wavelength of 514 nm and a spot size of 1 μm. The spectra were recorded with a 600 lines/mm grating. On quartz slides, optical transmittance spectra were collected in a UV solution u-4100 spectrophotometer. Transmittance properties were measured using a wavelength of 550 nm. Transmission electron microscopy (TEM, FET-Tecnai G2F20 S-7WIN) is a powerful tool to ascertain crystallographic information and also to determine the number of graphene layers[40]. Graphene films were transferred from the Cu and Ge substrates onto TEM grids by a PMMA-assisted wet-transfer method (Supplementary experimental details). The current–voltage (I–V) data were collected in ambient condition using Agilent (B1500A) semiconductor parameter analyzer. Measurements were performed in the range from −6 V to 6 V. The samples were soaked in 10 mL physiological saline (0.9 wt% NaCl aqueous solution) at 37°C for 72 h. After the immersion, the leaching liquid was collected respectively and then analyzed by inductively-coupled plasma mass spectrometry (ICP-MS; Nu Instruments, Wrexham, UK) to detect whether Cu, Ge, Si ions are released from the surfaces.

Antibacterial ability evaluation. The antibacterial activity of the graphene samples was evaluated by using Gram-negative E. coli (ATCC 25922) and Gram-positive S. aureus (ATCC 25923). After sterilization in 75 v/v% ethanol aqueous solution, a solution containing the bacteria at various concentrations of 10^7 CFU/mL, 10^6 CFU/mL and 10^5 CFU/mL was introduced onto the sample to a density of 60 μL/cm^2. The samples with the bacteria solution were incubated at 37°C for 24 h. The dissociated bacteria solution was collected and inoculated into a standard agar culture medium. After incubation at 37°C for 24 h, the culture plates with active bacteria were photographed according to the National Standard of China GB/T 4789.2 protocol. In order to resolve the potential problem of water evaporation from the bacterial solution, the remaining empty wells and the channels across the wells were filled with deionized water. Meanwhile, a container filled with deionized water was put on the bottom of the incubator. To ensure the validity of the results, the tests were repeated three times and each time three culture plates were used to seed each concentration of bacteria.

In order to perform fluorescence staining to show the viability of bacteria on the samples, bacteria at a concentration of 10^7 CFU/mL were inoculated on the samples mentioned above. Afterward, the culture medium was removed and the samples were rinsed with physiological saline, stained by using a LIVE/DEAD® BacLight™ Bacterial Viability Kit (L13152, Molecular Probes) for 15 min in dark, and then observed by fluorescence microscopy (Olympus GX71). In the SEM examination, a solution containing the bacteria at a concentration of 10^7 CFU/mL was put on the sample to a density of 60 μL/cm^2, incubated at 37°C for 24 h, fixed, and dehydrated in a series of ethanol solutions (30, 50, 75, 90, 95, and 100 v/v%) for 10 min each sequentially, with the final dehydration conducted in absolute ethanol (twice) followed by drying in the hexamethyldisilizane (HMDS) and ethanol solution series.

1. Novoselov, K. S. *et al.* Electric field effect in atomically thin carbon films. *Science* **306**, 666–669; DOI:10.1126/science.1102896 (2004).
2. Geim, A. K. & Novoselov, K. S. The rise of graphene. *Nat. Mater.* **6**, 183–191; DOI:10.1038/nmat1849 (2007).
3. Geim, A. K. Graphene: Status and prospects. *Science* **324**, 1530–1534; DOI:10.1126/science.1158877 (2009).
4. Bianco, E. *et al.* Stability and exfoliation of germanane: a germanium graphane analogue. *ACS Nano* **7**, 4414–4421; DOI:10.1021/nn4009406 (2013).
5. Mannoor, M. S. *et al.* Graphene-based wireless bacteria detection on tooth enamel. *Nat. Commun.* **3**, 763; DOI:10.1038/ncomms1767 (2012).
6. Nayak, T. R. *et al.* Graphene for controlled and accelerated osteogenic differentiation of human mesenchymal stem cells. *ACS Nano* **5**, 4670–4678; DOI:10.1021/nn200500h (2011).
7. Wang, G. *et al.* Direct growth of graphene film on germanium substrate. *Sci. Rep.* **3**, 2465; DOI:10.1038/srep02465 (2013).
8. Hu, W. *et al.* Graphene-based antibacterial paper. *ACS Nano* **4**, 4317–4323; DOI:10.1021/nn101097v (2010).
9. Akhavan, O. & Ghaderi, E. Toxicity of graphene and graphene oxide nanowalls against bacteria. *ACS Nano* **4**, 5731–5736; DOI:10.1021/nn101390x (2010).
10. Akhavan, O. & Ghaderi, E. Escherichia coli bacteria reduce graphene oxide to bactericidal graphene in a self-limiting manner. *Carbon* **50**, 1853–1860; DOI: http://dx.doi.org/10.1016/j.carbon.2011.12.035 (2012).
11. Salas, E. C., Sun, Z., Lüttge, A. & Tour, J. M. Reduction of graphene oxide via bacterial respiration. *ACS Nano* **4**, 4852–4856; DOI:10.1021/nn101081t (2010).
12. Kim, I. Y. *et al.* Strongly-coupled freestanding hybrid films of graphene and layered titanate nanosheets: an effective way to tailor the physicochemical and antibacterial properties of graphene film. *Adv. Funct. Mater.* DOI:10.1002/adfm.201303040 (2013).
13. Tu, Y. *et al.* Destructive extraction of phospholipids from Escherichia coli membranes by graphene nanosheets. *Nat. Nanotechnol.* **8**, 594–601; DOI:10.1038/nnano.2013.125 (2013).
14. Yu, Q. *et al.* Graphene segregated on Ni surfaces and transferred to insulators. *Appl. Phys. Lett.* **93**, 113103; DOI: http://dx.doi.org/10.1063/1.2982585 (2008).
15. Li, X. *et al.* Large-area synthesis of high-quality and uniform graphene films on copper foils. *Science* **324**, 1312–1314; DOI:10.1126/science.1171245 (2009).
16. Chen, S. *et al.* Oxidation resistance of graphene-coated Cu and Cu/Ni alloy. *ACS Nano* **5**, 1321–1327; DOI:10.1021/nn103028d (2011).
17. Singh Raman, R. K. *et al.* Protecting copper from electrochemical degradation by graphene coating. *Carbon* **50**, 4040–4045; DOI: http://dx.doi.org/10.1016/j.carbon.2012.04.048 (2012).
18. Dubey, G. P. & Ben-Yehuda, S. Intercellular nanotubes mediate bacterial communication. *Cell* **144**, 590–600; DOI: http://dx.doi.org/10.1016/j.cell.2011.01.015 (2011).
19. Harris, H. W. *et al.* Electrokinesis is a microbial behavior that requires extracellular electron transport. *PNAS* **107**, 326–331; DOI:10.1073/pnas.0907468107 (2010).
20. Reguera, G. *et al.* Extracellular electron transfer via microbial nanowires. *Nature* **435**, 1098–1101; DOI:10.1038/nature03661 (2005).
21. Lovley, D. R. *et al.* Humic substances as electron acceptors for microbial respiration. *Nature* **382**, 445–448; DOI:10.1038/382445a0 (1996).
22. Hartshorne, R. S. *et al.* Characterization of an electron conduit between bacteria and the extracellular environment. *PNAS* **106**, 22169–22174; DOI:10.1073/pnas.0900086106 (2009).
23. Eley, D. D. & Spivey, D. I. The semiconductivity of organic substances. Part 6.-A range of proteins. *Trans. Faraday Soc.* **56**, 1432–1442; DOI:10.1039/TF9605601432 (1960).
24. Du, J. *et al.* Hierarchically Ordered Macro-Mesoporous TiO_2-graphene composite films: improved mass transfer, reduced charge recombination, and their enhanced photocatalytic activities. *ACS Nano* **5**, 590–596; DOI:10.1021/nn102767d (2010).
25. Richardson, D. J. Bacterial respiration: a flexible process for a changing environment. *Microbiology* **146**, 551–571; DOI: http://mic.sgmjournals.org/content/146/3/551.short (2000).
26. Cassimeris, L., Lingappa, V. R. & Plopper, G. Lewin's Cells, 2nd Ed., Jones & Bartlett Publishers, Incorporated (2010).
27. Michaelson, H. B. The work function of the elements and its periodicity. *J. Appl. Phys.* **48**, 4729–4733; DOI: http://dx.doi.org/10.1063/1.323539 (1977).

28. Dimoulas, A., Tsipas, P., Sotiropoulos, A. & Evangelou, E. K. Fermi-level pinning and charge neutrality level in germanium. *Appl. Phys. Lett.* **89**, 252110–3; DOI: http://dx.doi.org/10.1063/1.2410241 (2006).
29. Romero, H. E. *et al.* n-Type behavior of graphene supported on Si/SiO_2 substrates. *ACS Nano* **2**, 2037–2044; DOI:10.1021/nn800354m (2008).
30. Alay, J. L. & Hirose, M. The valence band alignment at ultrathin SiO_2/Si interfaces. *J. Appl. Phys.* **81**, 1606–1608; DOI: http://dx.doi.org/10.1063/1.363895 (1997).
31. Williams, R. Photoemission of electrons from silicon into silicon dioxide. *Phys. Rev.* **140**, A569–A575; DOI: http://dx.doi.org/10.1103/PhysRev.140.A569 (1965).
32. Clarke, T. A. *et al.* Structure of a bacterial cell surface decaheme electron conduit. *PNAS* **108**, 9384–9389; DOI:10.1073/pnas.1017200108 (2011).
33. Dimroth, P., Kaim, G. & Matthey, U. Crucial role of the membrane potential for ATP synthesis by F(1)F(o) ATP synthases. *J. Exp. Biol.* **203**, 51–59; DOI: http://jeb.biologists.org/content/203/1/51.abstract (2000).
34. Brock, T. D. Milestones in Microbiology. *Academic Medicine* **36**, 847; DOI: http://journals.lww.com/academicmedicine/Fulltext/1961/07000/Milestones_in_Microbiology.51.aspx (1961).
35. Liu, S. *et al.* Antibacterial activity of graphite, graphite oxide, graphene oxide, and reduced graphene oxide: membrane and oxidative stress. *ACS Nano* **5**, 6971–6980; DOI:10.1021/nn202451x (2011).
36. Lyon, D. Y. *et al.* Antibacterial activity of fullerene water suspensions (nC_{60}) is not due to ROS-mediated damage. *Nano Lett.* **8**, 1539–1543; DOI:10.1021/nl0726398 (2008).
37. Tang, Y. J. *et al.* Charge-associated effects of fullerene derivatives on microbial structural integrity and central metabolism. *Nano Lett.* **7**, 754–760; DOI:10.1021/nl063020t (2007).
38. Lee, J. S., You, K. H. & Park, C. B. Highly photoactive, low bandgap TiO_2 nanoparticles wrapped by graphene. *Adv. Mater.* **24**, 1084–1088; DOI:10.1002/adma.201104110 (2012).
39. Ferrari, A. C. *et al.* Raman spectrum of graphene and graphene layers. *Phys. Rev. Lett.* **97**, 187401; DOI: http://dx.doi.org/10.1103/PhysRevLett.97.187401 (2006).
40. Moon, I. K., Lee, J., Ruoff, R. S. & Lee, H. Reduced graphene oxide by chemical graphitization. *Nat. Commun.* **1**, 73; DOI:10.1038/ncomms1067 (2010).

Acknowledgments

Joint financial support from the National Basic Research Program of China (973 Program, 2012CB933600), National Natural Science Foundation of China (81271704, 31100675, 31200721 and 31370962), Shanghai Science and Technology R&D Fund under grant 11JC1413700 and 13441902400 are acknowledged.

Author contributions

X.L. and Z.D. conceived and designed the experiments. J.L., G.W., H.Z., X.Z. and M.Z. performed the experiments and analyzed the data. J.L., G.W., X.L. and Z.D. co-wrote the manuscript. X.W. contributed to the data analysis and scientific discussion.

Additional information

Supplementary information accompanies this paper at http://www.nature.com/scientificreports

Competing financial interests: The authors declare no competing financial interests.

How to cite this article: Li, J.H. *et al.* Antibacterial activity of large-area monolayer graphene film manipulated by charge transfer. *Sci. Rep.* **4**, 4359; DOI:10.1038/srep04359 (2014).